Active site hydration governs the stability of Sn-Beta during continuous glucose conversion

Daniele Padovan‡, Luca Botti‡ and Ceri Hammond*

Cardiff Catalysis Institute, School of Chemistry, Cardiff University, Cardiff, CF10 3AT, United Kingdom

‡These authors contributed equally.

Supporting Information Placeholder

ABSTRACT: The stability of Sn-Beta for the continuous upgrading of hexoses is improved dramatically upon the addition of small amounts of water to the methanol/sugar reaction feed, despite water itself being an unfavourable solvent. Herein, the molecular level origin of this effect is investigated. Spectroscopic studies of the catalytic materials pre-, post- and during operation, with *operando* UV-Vis, ^{119}Sn CPMG MAS NMR, DRIFTS-MS, TGA, TPD/O-MS and porosimetry, are coupled to additional kinetic studies, to generate detailed structure-activity-lifetime relationships. In doing so, we find that the addition of water influences two particular processes – fouling and active site modification. However, mitigating the second is the most crucial role of water. Indeed, in the absence of water, the loss of Sn-OH and Si-OH sites occurs. Notably, these changes in active site hydration correlate to deactivation and reactivation of the system. The consequences of these findings, both for mechanistic understanding of the system in addition to the design of alternative regeneration methods, are also discussed.

Keywords: biomass upgrading, sugar conversion, zeolites, tin, *in situ* spectroscopy.

Introduction

The production of important commodity chemicals from renewable resources represents a focal point of contemporary chemical research.[1-5] Given their abundance and functionality, cellulose-based derivatives are the most viable source of carbon for the production of chemicals. Whilst several possible strategies exist for converting such feedstock into chemicals, selective catalytic methodologies offer several advantages, particularly in the context of process intensification. Of particular interest is the conversion of highly functionalised molecules such as glucose and fructose, which can be obtained following depolymerisation of cellulose. In this respect, the heterogeneous catalyst Sn-Beta (Sn-β) is of prime interest, having been shown to be highly active and selective for a range of processes such as i) fructose production *via* glucose-fructose isomerisation;[6-10] ii) the generation of renewable monomers such as alkyl lactates,[11,12] furanics[13,14] and methyl vinyl glycolate;[15-16] iii) the H_2-free reduction of carbonyl compounds *via* catalytic transfer hydrogenation;[17] and the Baeyer-Villiger oxidation of (renewable) ketones with H_2O_2 as oxidant.[18-20]

Possessing an ability to operate continuously, without exhibiting excessive levels of deactivation, is one of the most important properties a promising heterogeneous catalyst must exhibit, in order to be suitable for industrialization.[21,22] As such, study and optimization of the stability of the catalyst under continuous conditions is paramount. In contrast to fossil feedstock, the highly oxygenated nature of sugar-based substrates necessitates processing in the liquid phase. The addition of the solvent, alongside the chelating substrates present in solution, can dramatically impact the stability of a solid material, particularly when elevated pressures and temperatures are required for sufficient levels of macroscopic performance to be achieved.[23,24] As such, despite the significant interest in catalytic sugar upgrading, development of robust catalytic materials capable of continuous operation has lagged behind, prohibiting greater intensification.

Recently, we demonstrated that dramatic improvements to the stability of Sn-β during both glucose-fructose isomerisation, and the conversion of fructose to methyl lactate, could be achieved by adding small quantities of water to the conventional sugar/methanol feed, despite water itself being highly unfavourable as a solvent.[25] In fact, upon the addition of water (1-10 wt. %) to the feed, reactivity was found to increase by a factor of 2.5, and catalyst stability improved by one order of magnitude. Combined, these permitted continuous operation for up to 57 days without major losses in activity to be achieved.[25]

Herein, we investigate the molecular level origin of this surprising effect. Spectroscopic studies of the catalytic materials pre-, post- and during operation, with *operando* UV-Vis, ^{119}Sn CPMG MAS NMR, DRIFTS-MS, TGA, TPO-MS and porosimetry, are coupled to additional kinetic studies, to generate detailed structure-activity-lifetime relationships. These studies reveal that the addition of water primarily influences two distinct deactivation mechanisms. Firstly, its presence in the solution minimises the accumulation of carbonaceous residue within the pores of the zeolite, diminishing the extent of fouling. Additionally, water also prohibits loss of hydration of the isomorphously substituted Sn and Si atoms. Studies reveal that minimising the second of these processes is the dominant role of water, and that minimised fouling is, at most, only partially responsible for improved stability. The consequences of these findings, both with respect to mechanistic understanding of the system, in addition to the development of novel catalyst regeneration protocols, are also presented.

Results and Discussion

Kinetic observations. The continuous performance of Sn-β, containing between 2 and 10 wt. % Sn (henceforth denoted XSn-β where X represents the loading in wt. %) was examined for the low temperature isomerisation of glucose to fructose (henceforth

denoted GI) under benchmarked conditions.[25,26,27] To elucidate the impact of water, reactions were performed both in pure methanol (MeOH), and a mixture of water and methanol (10:90 w/w, henceforth denoted H_2O:MeOH). In contrast to previous studies,[25] all kinetic experiments were performed on undiluted catalyst samples, pressed and sieved to 63-75 μm, in order to aid spectroscopic study of the *ex reactor* samples by removing the typically employed diluent material (SiC). As can be seen (Table 1, Figure S1), the addition of small amounts of H_2O to MeOH significantly improves the stability of Sn-β at both high and low Sn loadings, with the rate of deactivation (k_d)[28] decreasing by a factor of six following its addition to the feed in both cases. These studies thus reveal that in addition to being observed in two different catalytic systems (GI and methyl lactate production[25]), the positive influence of water is observed irrespective of the precise Sn loading of the catalyst (2-10 wt. % Sn), further indicating that similar catalytic chemistry occurs in the material even at elevated loadings, in line with our previous research.[25]

Table 1. Rate of deactivation of 2Sn-β and 10Sn-β during continuous glucose isomerization in MeOH or H_2O:MeOH.

	Rate of deactivation / K_d ($X.h^{-1}$)	
Catalyst	MeOH	H_2O:MeOH
10Sn-β	0.016	0.0026
2Sn-β	0.028	0.005

Rate of deactivation calculated by the Levenspiel method.[28]

Characterisation of textural properties. To elucidate the molecular level origin of the water effect, structure-activity-lifetime relationships were generated, primarily for samples of 10Sn-β following operation in MeOH or H_2O:MeOH for 50-60 h. Over this time period, the catalyst exhibited approximately 55 and 5 % loss of activity in MeOH and H_2O:MeOH, respectively. Since the catalyst retains crystallinity during this period of operation,[25,26] preliminary characterisation studies of the undiluted, *ex reactor* samples were performed with TGA, TPO-MS and ^{13}C MAS NMR. TGA (Figure S2) and TPO-MS (Figure 1, Left) studies indicate that multiple species are lost during thermal treatment of the used catalytic samples, with both methanol and CO_2 detected during analysis of the effluent. In terms of the CO_2 released, control experiments performed by solvothermally treating the catalyst in MeOH and H_2O:MeOH for identical periods of time indicate that a large fraction of these residues arise from the solvent alone (Figure S3). This agrees well with ^{13}C MAS NMR analyses, which indicate that only one detectable resonance (δ = 49.8 ppm) is observed in all used samples, characteristic of retained methanol (Figure 1, Right). Accounting for the fact that each retained sugar molecule provides six-times more CO_2 during TPO, and that only one resonance is observed by MAS NMR, it is evident that the major species retained in the catalyst after reaction arise from the solvent. Even so, it is clear that that the total type and quantity of this retained carbon is diminished when water is co-added to the reaction feed.

Given that pore fouling is an established form of Sn-β deactivation,[29] it is possible that the decrease in the quantity of carbonaceous residues in the co-presence of water may minimise the contribution of fouling to deactivation. Consequently, porosimetry analysis of the partially deactivated samples was also performed (Table 2). Interestingly, both samples exhibit a loss of porosity following continuous operation. However, a direct correlation between remaining porosity of the sample and the extent of activity loss is not evident, as both samples lose approximately 15-25 % pore volume during this operational period. Although it cannot be ruled out that deactivation arises from the retention of a specific type of residue, and/or blockage of a particular type of active site, these measurements already suggest that minimised pore fouling is not the dominant role of water.

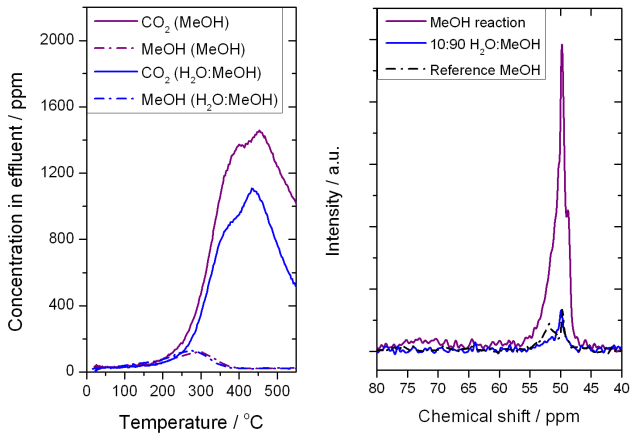

Figure 1. (Left) TPO-MS measurements from Sn-β following reaction in MeOH and H_2O:MeOH. The evolution of MeOH and CO_2 are displayed. (Right) ^{13}C MAS NMR analysis of Sn-β following GI in MeOH and H_2O:MeOH.

Table 2. Porosity data for various stannosilicate catalysts prior to, and following, continuous operation for GI.

Entry	Catalyst	SSA ($m^2\ g^{-1}$)	V_{micro} ($cm^3\ g^{-1}$)	Activity lost (%)
1	10Sn-β pelletized (63-75 μm)	351	0.226	-
2	10Sn-β used in MeOH	279	0.178	55
3	10Sn-β used in H_2O:MeOH	294	0.192	5

Porosity data determined by N_2 isotherms; Brunauer-Emmett-Teller surface area (S_{BET}) calculated from BET method, and micropore volume (V_{micro}) derived from the t-plot method.

Site selective spectroscopic methods. In addition to pore fouling, the loss and/or reorganisation of active sites is also a primary cause of zeolite deactivation. To gain further insight regarding the impact of water, site selective spectroscopic studies were thus performed. Given its sensitivity to the active sites of the catalyst, in addition to other chromophoric species that could be formed during the reaction, UV-Vis spectroscopy represents a powerful method of gaining insight into the impact of water.[30] However, to maximise the scientific rigour of the analysis, UV-Vis analysis was performed *in operando*, following development of a continuous reactor capable of permitting UV-Vis spectra to be collected throughout continuous operation of the catalyst (so called *operando* spectroscopy).[31-35] Notably, measuring the absorption spectra *in operando* permits the rate of evolution of each band to be correlated against real kinetic performance. Importantly, the kinetic data obtained from this reactor was identical to that obtained for the same system in a conventional reactor (Figure S4). To aid comparison, spectra are shown in "difference" mode, background

subtracted to the spectra of the fresh catalyst recorded at the beginning of each reaction. Accordingly, positive signals represent absorption features gained during the reaction, whilst negative signals represent those features lost during reaction. Preliminary control experiments, performed by treating Sn-β and dealuminated β with various reactants under otherwise operational conditions for 1 h on stream, revealed the following: (1) All chromophoric changes were related to Sn *i.e.* in the absence of Sn, no absorption changes were observed; (2) Interaction between Sn and pure methanol results in the formation of two positive absorption features (260 nm and 315 nm), and a negative absorption signal at 223 nm; and (3) interaction between Sn and glucose results in absorptions at 341 and 440 nm (Figure 2). We note that the contact time in each reaction was adjusted so that both systems presented an initial conversion of ± 40 %, to ensure both reactions were monitored over similar stages of the reaction coordinate.[21]

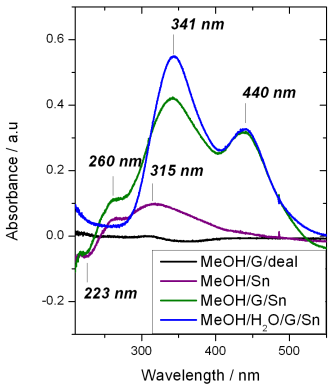

Figure 2. Control samples performed for assignment of UV-Vis spectra, achieved by dosing 10Sn-β and dealuminated β with pure methanol (MeOH), methanol/glucose (MeOH/G) and methanol/water/glucose (MeOH/H_2O/G) solutions.

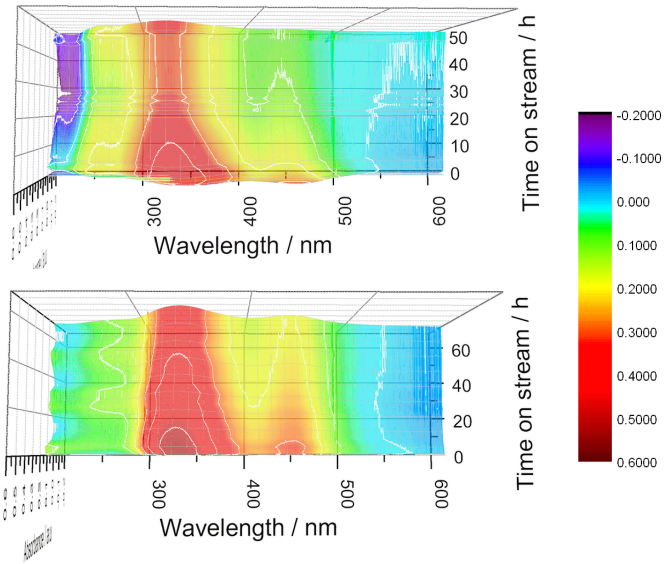

Figure 3. Difference UV-Vis spectra of 10Sn-β during GI in (top) MeOH, and (bottom) H_2O:MeOH. Spectra were recorded *in operando* (110 °C, 10 bar backpressure, $X_{GLU(0)}$ = 40 %).

Figure 3 presents the difference spectra of 10Sn-β during GI in MeOH (top) and H_2O:MeOH, by collection of the absorption spectra *in operando*. As expected from control experiments, the 300-450 nm region rapidly increases in absorbance during the very early stages of both reactions, due to the interactions between Sn-methanol (315 nm) and Sn-glucose (341, 440 nm). Interestingly, intensity in this region is slightly higher when water is present, possibly indicating preferential transport of glucose to Sn in the co-presence of water. In MeOH, intensity above 350 nm diminishes after approximately 10 h on stream, where as in 10:90 H_2O:MeOH, the intensity remains largely consistent until longer times on stream. The lower energy Sn-glucose feature (440 nm) is also present at the very early stages of both catalytic reactions. However, its intensity diminishes rapidly in both systems, particularly so in pure methanol.

An obvious difference in the high-energy region of both systems is also evident. Indeed, whilst intensity in the high energy region (210-300 nm) remains relatively constant in H_2O:MeOH, a decrease in intensity at 223 nm and an increase in intensity at 260 nm is observed when the reaction is performed in MeOH. Interestingly, the degree of change in this region also correlates to time on stream in both systems, remaining relatively consistent in H_2O:MeOH, but gradually increasing in magnitude throughout the operational period in MeOH as the catalyst suffers deactivation.

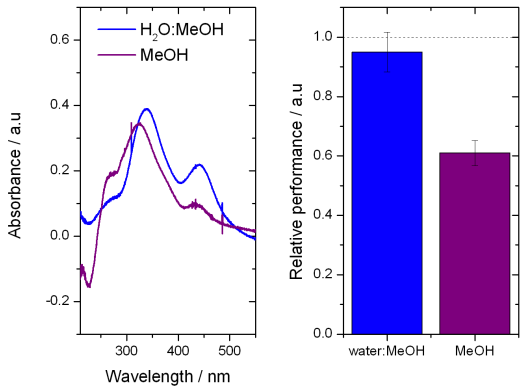

Figure 4. (Left) Difference UV-Vis spectra of 10Sn-β during GI in MeOH and H_2O:MeOH at 25 h on stream, and (Right) Relative performance of 10Sn-β for GI in MeOH and H_2O:MeOH at 25 h.

To better compare the impact of these changes, particularly with respect to kinetic performance, the difference spectra of each reaction, collected at 25 h on stream, is presented in Figure 4 Left, alongside the relative performance of the catalyst in both systems at that same point in time (Figure 4, Right). When correlated to the performance of the catalyst over both operational periods (Figure 3), in addition to the relative performance of the catalyst in both solvents at one fixed point in time (Figure 4), it is clear that only two of the changes correlate to loss of activity. These include the change of intensity in the high energy region (decrease at 223 nm, increase at 260 nm), in addition to the decrease in intensity between 350-400 nm. Crucially, the absence of water is essential for these spectral changes to occur, and each change occurs at similar time periods of the reaction in MeOH.

As control studies indicate that the changes in the high energy region arise from interaction of the catalyst with pure methanol (Figure 2), the ability of the solvent alone to diminish the activity of 10Sn-β was investigated. To do so, GI was performed after solvothermally treating 10Sn-β in pure methanol for 24 h prior to operation *i.e.* glucose was introduced into the feed after treating the catalyst in methanol for 24 h at 110 °C and 10 bar of back-

pressure. As can be seen (Figure 5), the starting conversion obtained after treating the catalyst in methanol for 24 h (18 %) matches the conversion value obtained after continuous operation of the catalyst over the same period of time, even though no glucose has passed over the catalyst during the first 24 h. This strongly indicates that changes occurring to Sn^{4+} due to the solvent, and not factors related to the presence of substrate, are the primary reasons for catalyst deactivation.

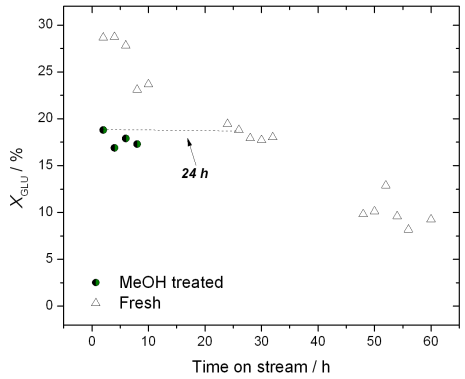

Figure 5. Catalytic performance of 10Sn-β for GI in MeOH as a fresh catalyst (black squares) and after a 24 h pre-treatment period in methanol.

The high energy region of the UV-Vis spectra is related to the ligand-to-metal charge transfer (LMCT) bands of the Sn^{4+} sites of the catalyst.[36] Hence, changes in this spectral region relate to changes to the coordination sphere of Sn^{4+}, possibly through ligand exchange, and/or changes in its speciation, such as its agglomeration into oxidic particles. Thus, to better understand the changes that occur to the Sn sites of the zeolite during operation, ^{119}Sn MAS NMR experiments were performed.[37-38] In line with recent developments, spectra were recorded by Carr-Purcell-Meiboom-Gill (CPMG) echo-train acquisition methods, as exemplified by the Ivanova group.[39,40] Due to the signal enhancements made possibly by CPMG methods, spectra could be recorded on materials containing naturally abundant quantities of Sn. All *ex reactor* samples were measured without prior heat treatment, in order to preserve integrity of the samples following operation, and were thus compared to fresh samples also in their hydrated forms.

Figure 6 Left presents the direct excitation CPMG (DE-CPMG) ^{119}Sn MAS NMR spectrum of 10Sn-β prior to reaction (a), and following 50 h of reaction in MeOH (b) and H_2O:MeOH (c). Given differences in t_1 relaxation times, precise quantification of the percentage of each species is not possible. Indeed, we note that measurement of samples with a recycle delay time of only 2s dramatically under-represents the quantity of isomorphously substituted Sn (Figure S5). However, systematic comparison prior to, and following reaction, still allows a (semi)-quantitative insight of the changes in speciation that occur, provided identical acquisition methods are employed.

Four dominant resonances are observed in the fresh catalyst, at chemical shifts of -705, -655, -600 and -541 ppm. The presence of multiple signals indicates the presence of multiple Sn species, and is a consequence of the high Sn loading of the sample (10 wt. % Sn). In fact, the signals at -541 and -600 ppm are indicative of pentacoordinated Sn and extra-framework (inactive) SnOx species, respectively,[40] which we have previously demonstrated to be spectators during catalytic operation.[41] As further evidence of this, we refer to Table 1 and Figure S1, which demonstrate the same kinetic phenomena in the presence of water is observed irrespective of the loading of Sn employed. In addition to these signals, two major resonances at -655 and -705 ppm are also observed. Resonances at these chemical shifts are typically assigned to the framework Sn sites of the catalyst in their hydrated form *i.e.* octahedral, framework Sn sites.[42-44] However, as the precise chemical shift of these species depends on multiple factors, including T-site occupation, degree of Sn, the number and type of proximal defects, in addition to the exact method of analysis, we simplistically treat both resonances as one type of site, that being octahedrally coordinated framework Sn^{4+} sites in a hydrated state. Notably, analysis of 1Sn-β, possessing only 1 wt. % Sn but exhibiting a two-fold higher turnover frequency *i.e.* activity per gram of Sn,[41] indicates that the species responsible for the signal at -705 ppm is likely the most important site, as the relative intensity of this signal dominates at lower loadings when the highest levels of TOF are obtained (Figure S6).

Following continuous operation in MeOH (b) and H_2O:MeOH (c), only minor changes to the Sn sites are observed by DE-CPMG (Figure 6, Left). Most notable amongst these is the relative growth in intensity for the -600 ppm signal, and a small increase in the relative ratio of the -655 to the -705 ppm signal. These indicate the formation of some additional, inactive, SnOx sites, in addition to minor modification to the T sites of the catalyst, respectively. Although it is not possible to quantify the extent of this restructuring within each particular sample (*Vide Supra*), it is evident that these changes are almost identical in both systems, despite the dramatic differences in relative activity after 50-60 h on stream. Hence, these changes clearly do not correlate to decreased performance, which is much more dramatic in MeOH. This also indicates that the formation of extra-framework SnOx is not the only reason behind the increase in absorption at 260 nm during continuous operation in MeOH (Figure 4), as this absorption signal does not form during continuous operation in H_2O:MeOH despite a similar amount of SnOx forming during this reaction. Taken together, DE-CPMG indicates that the same types of Sn species are mainly present in the catalytic material after reaction regardless of the choice of solvent. This rules out dramatic changes to the Sn site speciation as being the primary reason for deactivation.

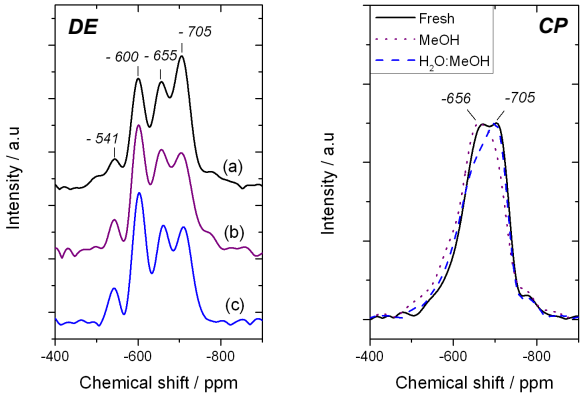

Figure 6. (Left) ^{119}Sn DE-CPMG MAS NMR spectra of 10Sn-β prior to (a) and following reaction in MeOH (b) and H_2O:MeOH (c). (Right) ^{119}Sn CP-CPMG MAS NMR spectra of 10Sn-β prior to and following reaction in MeOH and H_2O:MeOH.

In contrast, clear differences in both *ex reactor* samples can be identified when cross polarisation (^{1}H-^{119}Sn, CP-CPMG) methods are employed (Figure 6, Right). In the fresh sample, both signals between -655 and -700 ppm are clearly amenable to cross polarisation, indicating both Sn species have protons in their vicinity. However, a clear decrease in the signal at -705 ppm is observed following reaction in pure methanol. This indicates that the pro-

ton(s) in the vicinity of this particular Sn species are lost during reaction. Notably, this effect only occurs when water is absent, since the -705 ppm signal remains present following reaction in H_2O:MeOH, where very little deactivation is observed. Considering that the relative ratio between the -655 and -705 ppm signals does not change dramatically following both reactions, as evidenced by DE-CPMG, complimentary CP-CPMG studies indicate that it is the environment that surrounds the Sn sites that changes in the absence of water. As the -705 ppm signal is dominant at lower loadings (Figure S6), when the highest levels of intrinsic activity are observed, changes to the environment of this species are likely to lead to consequences for kinetic performance.

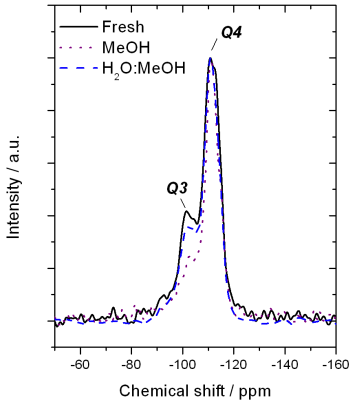

Figure 7. ^{29}Si MAS NMR of Sn-β, prior to reaction, and following GI in MeOH and 10:90 H_2O:MeOH.

According to previous studies, the formation of Sn-OH species following interaction of Sn-β with water, is also accompanied by the formation of Si-OH groups, particularly at the reaction temperatures employed in this study.[45] In good agreement to this, it is notable that both the fresh catalyst, and used sample following reaction in H_2O:MeOH, exhibit Q3 resonances (-103 ppm) in the ^{29}Si MAS NMR spectra, indicating the presence of Si-OH groups (Figure 7).[46] However, a much lower signal at this chemical shift was observed in the used sample obtained after reaction in MeOH. The absence of this signal indicates that the absence of water also permits the loss of Si-OH to occur, analogously to the loss of the Sn-OH. Given that the loss of these protons is only observed following substantial deactivation of the catalyst in pure methanol, it is clear that keeping hydration in the active site environment by maintaining the presence of some water is essential for stability to be maintained. Since water is known to more readily adsorb to Sn-β compared to other substrates, such as NH_3, alcohols and acetonitrile,[47-49] this may account for the positive effect of water even when present at low levels (1 wt. %).[25]

The loss of Si-OH and Sn-OH protons could be attributed to ligand exchange at the active site *i.e.* the displacement of coordinated water for methanol and/or alkoxylation of a putative Sn-OH bond with methanol, or alternatively to (re-)condensation of the structure, with the (re-)formation of Sn-O-Si bonds. Although no concrete methodologies for identifying Sn-OH exist, and hence direct differentiation of these pathways is not feasible, spectroscopic studies with DRIFTS reveal the formation of metal-alkoxylates to be at least partially responsible for the loss of signal (Figure 8). Indeed, treating Sn-β with various alcohol probe molecules (methanol, d^4-methanol, ethanol, isoproponal) at 110 °C results in the formation of new vibrational signals that are sensitive both to the presence of Sn, in addition to the reduced mass of the R-OH probe molecule (Figure 8 Right, Figures S7-S8). Whilst this observation does not rule out a contribution from framework condensation (Sn-O-Si formation) during the reaction, it clearly indicates that the formation of Sn-alkoxy species is at least partly responsible for the loss of Sn-OH and Si-OH species. We note that such species were previously hypothesised by the group of Roman-Leshkov.[50] Notably, flushing the DRIFTS cell with water following formation of the Sn-alkoxy species results in its removal from the DRIFTS spectrum, even when a large amount of physisorbed methanol is still present in the sample (Figure S9). These observations indicate both the reversibility of alkoxy formation, in addition to the preferential binding of water over methanol.

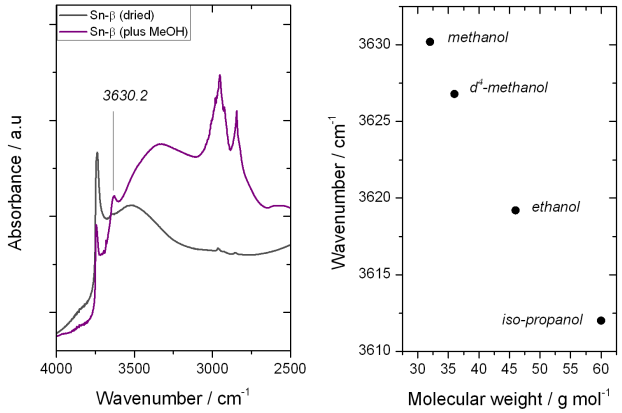

Figure 8. (Left) DRIFTS spectra of Sn-β following dosing with methanol at 110 °C. (Right) Influence of molecular weight of the R-OH probe on the final vibrational wavenumber of the new vibration.

Kinetic confirmation of active site hydration effects. *Operando* UV-Vis, ^{119}Sn CPMG MAS NMR, ^{29}Si MAS NMR and DRIFTS studies indicate that deactivation of the catalyst in the absence of water is accompanied by the loss of Sn-OH and Si-OH species, at least partly due to ligand exchange at the active site. The loss of these sites could lead to deactivation through two distinct means. Firstly, maintaining hydration at the active site and its vicinity may simply favour the transportation of sugars to and from the active site (transport hypothesis). An alternative role of hydration may be the stabilisation of a more intrinsically active Sn site (kinetic hypothesis). For example, several studies have reported that the open form of Sn-β, where one or more Sn-OH and Si-OH bonds are present due to partial hydrolysis of the framework, is the most active form of the catalyst.[51] In fact, theoretical studies have hypothesised that the temperature dependence of Sn-β increases by approximately 30 kJ mol^{-1} when the site is fully closed, due to the loss of proximal Si-OH species that can contribute to H-bonding of the substrate.[52,53]

To conclusively differentiate between the kinetic and transport hypotheses, an additional series of kinetic experiments focused on determining the temperature dependence of the catalyst at various stages of deactivation was performed. If the system becomes limited by the uptake of glucose, the reaction should exhibit very low temperature dependence, indicative of transport limitations. In contrast, the formation of a less active Sn site should result in an increase in the temperature dependence of the system, relative to the fresh catalyst. Finally, no change in the temperature dependence of the system would simply indicate that the same active sites are present, but that their concentration is lower, due to the formation of inactive (spectator) Sn species. Figure 9 Left, presents the effective temperature dependence of the fresh catalyst, and that of the catalyst following solvothermal treatment in methanol for 24 h. As can be seen, following pre-treatment of the sam-

ple in pure methanol for 24 h, which induces approximately 35 % deactivation (Figure 5), the apparent temperature dependence of the reaction increases substantially, from 39 to 67 kJ mol^{-1} (Figure 9, Left). The increase calculated from experiment (28 kJ mol^{-1}) is in excellent agreement to the increase predicted from theory to occur following the loss of cooperating Sn-OH and Si-OH sites, further indicating the loss of hydrated active sites.[52,53]

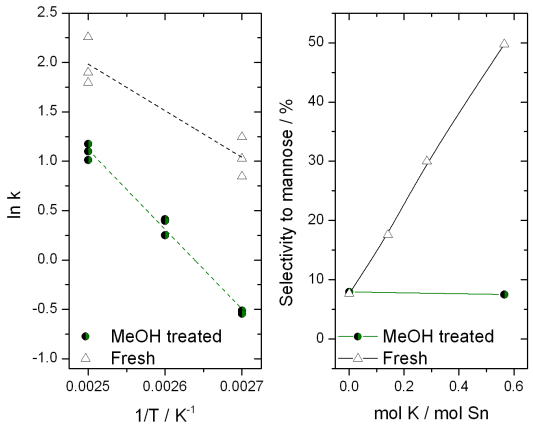

Figure 9. (Left) Apparent temperature dependence of fresh 10Sn-β, and 10Sn-β pre-treated in pure methanol for 24 h prior to operation. A contact time of 0.19 minute was employed throughout both experiments, and temperatures of 100, 110 and 120 °C were used. (Right) Influence of K_2CO_3 on the selectivity to mannose (epimerisation product) during GI at 110 °C in pure methanol. 10Sn-β, and 10Sn-β pre-treated in pure methanol for 24 h prior to operation, were used as catalysts.

To further verify the hypothesis that it is the loss of Si-OH and Sn-OH that results in diminished performance, the influence of alkali exchange was examined (Figure 9, Right). Indeed, several experimental studies have demonstrated that ion-exchange of Sn-β with alkali salts can dramatically impact its selectivity performance. For GI, ion-exchange has been shown to result in switch in reaction selectivity, with epimerisation to mannose dominating in the presence of alkali metals, as opposed to the classical isomerisation to fructose in the absence of such additives.[54,55] Likewise, ion-exchange at these positions during ML production results in an increased selectivity to retro-aldol product formation.[12] As can be seen (Figure 9, Right), whereas the presence of K_2CO_3 results in a dramatic increase in mannose selectivity for the fresh catalyst, the methanol-treated sample is not modified by the presence of alkali (Table S1-S2). This strongly indicates the absence of ion-exchangeable Si-OH and Sn-OH species following partial deactivation of the catalyst, in excellent agreement to the spectroscopic and kinetic evidence.

Regeneration studies. From the spectroscopic and kinetic experiments presented above, it is clear that deactivation of the catalyst relates to the loss of Sn-OH and Si-OH species in the absence of water. Since the dissociative adsorption of water, and the concurrent formation of Sn-OH and Si-OH species, is reportedly rapid when Sn-β is exposed to water,[45] it was hypothesised that activity should be restored in deactivated samples through simple solvothermal treatment of the sample (low temperature regeneration). According to this hypothesis, the loss of Si-OH and Sn-OH should be reversible by re-introducing water into the feed, without the need for classical high temperature thermal treatment being performed. To probe this, a variety of washing protocols on partially deactivated samples of Sn-β were performed, following an initial cycle of GI in methanol for 60 h. As can be seen (Figure 10), solvothermally treating a partially deactivated sample of 10Sn-β allows initial catalytic activity to be fully restored. Interestingly, the regeneration is sensitive to the solvent of choice, in addition to the time of treatment (12 h *vs.* 20 h). Indeed, whereas a solution of H_2O:MeOH is able to fully restore catalytic activity within 20 h, employing methanol alone results in no recovery being achieved. This is in agreement to conclusion that it is methanol that is the primary cause of deactivation. Interestingly, when water alone is employed as wash solution, no regeneration is observed, even when the time of treatment is adjusted so that the same total quantity of water is flowed over the partially deactivated catalyst (2 h versus 20 h). This clearly emphasises the need to optimise the concentration of water, in order to balance active site recovery against amorphisation of the framework, which is known to occur in bulk water at these temperatures.[26]

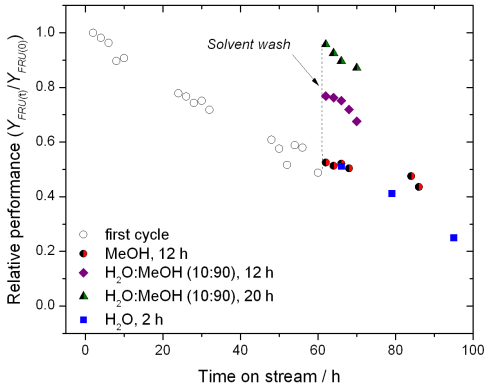

Figure 10. Low temperature, solvothermal regeneration of Sn-β, following an initial cycle of GI in pure methanol. Second cycles were also performed in pure methanol.

Table 3. Porosimetry data for various Sn-β catalysts prior to, and following, solvothermal regeneration**.**

Entry	Catalyst	V_{micro} (cm^3 g^{-1})
1	Fresh 10Sn-β pellet	0.226
2	10Sn-β, used in pure MeOH for 50 h	0.178
3	used 10Sn-β, after washing in H_2O:MeOH	0.218
4	used 10Sn-β, after washing in MeOH	0.198

Porosity data determined by N_2 isotherms; Brunauer-Emmett-Teller surface area (S_{BET}) calculated from BET method, and micropore volume (V_{micro}) derived from the t-plot method.

To gain a better understanding of the regeneration process, and hence to gain additional indirect insight regarding the mechanism(s) of deactivation, spectroscopic studies of the catalyst following regeneration were performed (Table 3). Porosimetry revealed that washing the sample in H_2O:MeOH restored a large fraction of pore volume, indicating removal of the carbonaceous residue. This is in good agreement to the observation that the presence of water in the feed results in decreased retention of residue (Figure 1, Table 2). Notably, although regeneration of the

catalyst does not occur by treating the sample in MeOH alone, a large fraction of the lost pore volume is still recovered by this treatment. The fact that carbonaceous residue is removed without regeneration being observed further indicates that the accumulation of such residue, and pore fouling in general, is not the primary cause of deactivation, and that the removal of such residue is not the primary role of water.

To verify whether solvothermal regeneration of the catalyst results in restoration of the hydrated state of the catalyst, additional ^{119}Sn CP-CPMG MAS NMR and UV-Vis measurements on the regenerated sample were performed (Figure 11). As can be seen, regeneration of the sample in H_2O:MeOH results in regeneration of both the signal at -705 ppm in the ^{119}Sn CP-CPMG MAS NMR spectrum, in addition to reversal of the high energy changes in the UV-Vis spectra, both of which correlate to decreased kinetic performance. We highlight that the ability to regenerate the catalyst without resorting to classical high temperature (> 550 °C) thermal treatment also represents a major breakthrough, as solvothermal treatment of the catalyst means the reactor does not to be drained prior to regeneration, reduces overall energy input, and negates the requirement for high temperature heating provision.

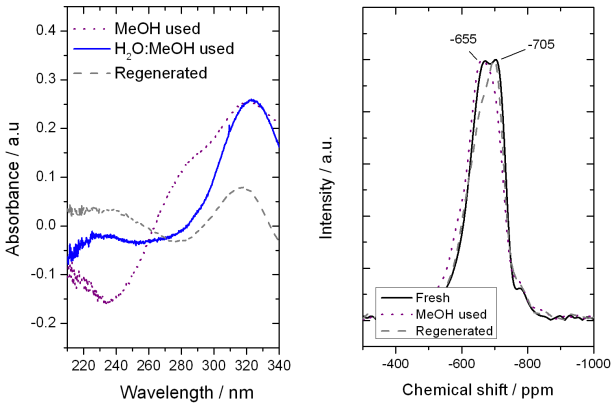

Figure 11. (Left) UV-Vis of 10Sn-β deactivated in MeOH (purple dotted line), 10Sn-β deactivated in H_2O:MeOH methanol (blue solid line) and following regeneration of 10Sn-β in H_2O:MeOH (grey dashed line). (Right) ^{119}Sn CP-CPMG MAS NMR spectra of fresh 10Sn-β prior to (black), following reaction in pure methanol (purple) and following regeneration in H_2O:MeOH (grey).

Conclusions

This study focuses upon elucidating the molecular level origin of how small amounts of water are able to mitigate deactivation during the continuous conversion of sugars to chemicals. Spectroscopic studies of the catalytic materials pre-, post- and during-operation, with *operando* UV-Vis, ^{119}Sn and ^{29}Si CPMG MAS NMR, DRIFTS-MS, TGA, TPO-MS and porosimetry, coupled with detailed kinetic studies of these systems, reveal that the addition of water primarily influences the rate deactivation of Sn-Beta by two distinct mechanisms. Firstly, its presence in the solution minimises the accumulation of carbonaceous residue within the pores of the zeolite, minimising contributions from fouling. Additionally, its presence also minimises changes to the coordination sphere and the hydration state of isomorphously substituted Sn and Si. Combined, these studies reveal that minimising the loss of Sn-OH and Si-OH species is the dominant role of water, and that its addition to the feed maintains hydration of the active site environment. Although water also minimises fouling, this processes is, at most, only partially responsible for improved stability. Based on these findings, novel regeneration protocols, based on solvothermal washing of deactivated catalysts, are also presented. Given the benefits associated with regenerating samples without resorting to classical high temperature thermal treatment, future work will study the washing regeneration process in greater detail, with the aim of identifying its suitability as a replacement for conventional thermal regeneration for other Sn-β catalysed reactions.

Experimental details

Catalyst synthesis

A commercial zeolite Al- β (Zeolyst, NH_4^+-form, Si/Al = 19) was dealuminated by treatment in HNO_3 solution (13 M HNO_3, 100 °C, 20 mL g^{-1} zeolite, 20 hours). Solid-state stannation of dealuminated zeolite β was performed the procedure reported in reference 44, by grinding the appropriate amount of tin(II) acetate with the necessary amount of dealuminated zeolite for 10 minutes in a pestle and mortar. Following this procedure, the sample was heated in a combustion furnace (Carbolite MTF12/38/400) to 550 °C (10 °C min-1 ramp rate) first in a flow of N_2 (3 h) and subsequently air (3 h) for a total of 6 h. Gas flow rates of 60 mL min^{-1} were employed at all times.

Kinetic studies

Continuous GI reactions were performed in a plug flow, stainless steel, tubular reactor. The reactor was connected to an HPLC pump in order to regulate the reactant flow and allow operation at elevated pressures. The catalyst was pelleted and particle size comprised between 63 and 77 μm were selected and placed in between two plugs of quartz wool. The catalyst was densely packed into a ¼" stainless steel tube (4.1 mm internal diameter), and a frit of 0.5 μm was placed at the reactor exit. The reactor was subsequently immersed in a thermostatted oil bath at the desired reaction temperature. Pressure in the system was controlled by means of a backpressure regulator, typically set at 10 bar, in order to allow operations above the boiling temperature of the solvent. Aliquots of the reaction solutions were taken periodically from a sampling valve placed after the reactor and analysed by an Agilent 1260 Infinity HPLC equipped with a Hi-Plex Ca column and ELS detector and quantified against an external standard (sorbitol) added to the sample prior the injection.

Solvothermal regeneration of the catalytic bed was performed by changing the reactor feed to the desired solvent or solvent mixture, which was flowed through the bed for a certain amount of time. The treatment was carried out at the same flow rate and the same temperature at which the reaction was performed (110 °C). Subsequently, the reactor feed was switch back to the reactant solution and a second cycle was performed.

GI batch studies were performed in a pressurised Ace tubular glass reactor thermally controlled by a hot oil bath on an IKA hot plate. 5 g of reactant solution (1 wt. % glucose in methanol), catalyst and K_2CO_3 (where required) were placed inside the reactor in order to fix the glucose/Sn and K^+/Sn molar ratio to 50 and 0.5 respectively. Samples were periodically collected and analysed by HPLC as described above.

Catalyst Characterisation

Specific surface area was determined from nitrogen adsorption using the BET equation, and microporous volume was determined from nitrogen adsorption isotherms using the t-plot method. Porosimetry measurements were performed on a Quantachrome Quadrasorb, and samples were degassed prior to use (115 °C, 6h,

nitrogen flow). Adsorption isotherms were obtained at 77 K. TGA analysis was performed on a Perkin Elmer system. Samples were held isothermally at 30 °C for 30 minutes, before being heated to 550 °C (10 °C min^{-1} ramp rate) in air. TPO-MS measurements were performed on a home-made system formed by a Bruker Tensor II equipped with a Harrick praying mantis DRIFT cell, connected with a Hiden QGA Mass Spectrometer. A weighed amount of catalyst was placed inside the DRIFT cell and its surface was constantly monitored by the IR spectrometer. The cell was heated from 30 to 550 °C (ramp rate 10 °C/min) and a constant flow of air was used throughout the experiment (10 mL min^{-1}). The outlet of the cell was connected to a mass spectrometer for the online analysis of the effluent. Operando UV-Vis measurements were performed with a home made tubular reactor equipped with fibre optic UV-Vis probe. UV-Vis measurements were performed with a light source (Ocean Optics DH-2000), spectrometer (Maya 2000 Pro, Ocean Optics) and a 600 µm UV-Vis fibre. The light was directed onto an optically transparent reactor column, located within a heated aluminium block. *Ex situ* UV-Vis were performed in a similar manner, with the exception that the fibre was focused directly on the powder samples. MAS NMR analysis was performed at Durham University through the National solid-state NMR service. All the samples were non-enriched and were measured on a Bruker Avance III HD spectrometer at operating frequencies of 400, 100, 149 and 79 MHz for ^{1}H, ^{13}C, ^{119}Sn and ^{29}Si, respectively. Typically, between 50-100 mg of solid sample was packed in a 4 mm rotor and spun at ± 12,000 Hz. For ^{119}Sn MAS NMR, samples were measured by the CMPG method as described in references 39 and 40. Spectra were acquired both in direct excitation and cross polarisation modes. Recycle delay times of 1 and 2 seconds was applied for ^{119}Sn CP CPMG MAS NMR and ^{119}Sn DE CPMG MAS NMR, respectively. DRIFT spectroscopy analyses were performed in Harrick praying mantis cell. The spectra were recorded on a Bruker Tensor Spectrometer over a range of 4000-650 cm^{-1} at a resolution of 2 cm^{-1}. Alcohol adsorption studies with DRIFT spectroscopy were performed on the pre-treated zeolite powder (heated to 110 °C for 30 min in nitrogen at 40 mL min^{-1} prior to adsorption). The alcohol was dosed by passing the gas stream through a saturator module. Samples were maintaining at 110°C during the experiment to simulate reaction conditions. Spectra were recorded after 20 min of absorption.

ASSOCIATED CONTENT

Supplementary information, containing additional kinetic and spectroscopic details is available. The Supporting Information is available free of charge as a PDF on the ACS Publications website.

AUTHOR INFORMATION

Corresponding Author

E-mail: hammondc4@cardiff.ac.uk; Tel: +44 (0) 29 2087 6002

ACKNOWLEDGMENTS

CH gratefully appreciates the support of The Royal Society, for provision of a University Research Fellowship (UF140207). CH and LB are grateful to Haldor Topsøe A/S for further research funding. Dr. Esben Taarning, Dr. Irantzu Sádaba, Dr. Søren Tolborg and Dr. Juan Salvador Martinez Espin, all from Haldor Topsøe A/S, are thanked for fruitful discussions and support. Dr. David Apperley (Durham University) is acknowledged for support with MAS NMR measurements. Massimiliano Caiti is also thanked for experimental support.

REFERENCES

(1) Delidovich, I.; Leonhard, K.; Palkovits, R. Cellulose and Hemicellulose Valorisation: An Integrated Challenge of Catalysis and Reaction Engineering. *Energy Environ. Sci.* **2014**, 2803–2830.

(2) (2) Tuck C. O.; Pérez, E.; Horváth I. T.; Sheldon R. A.; Poliakoff M. Valorization of Biomass: Deriving More Value from Waste. *Science* **2012**, 695-700.

(3) Zhang, X.; Wilson, K.; Lee, A. F. Heterogeneously Catalyzed Hydrothermal Processing of C5-C6 Sugars. *Chem. Rev.* **2016**, 12328–12368.

(4) Ennaert, T.; Van Aelst, J.; Dijkmans, J.; De Clercq, R.; Schutyser, W.; Dusselier, M.; Verboekend, D.; Sels, B. F. Potential and Challenges of Zeolite Chemistry in the Catalytic Conversion of Biomass. *Chem. Soc. Rev.* **2016**, 584–611.

(5) Climent, M. J.; Corma, A.; Iborra, S. Conversion of Biomass Platform Molecules into Fuel Additives and Liquid Hydrocarbon Fuels. *Green Chem.* **2014**, 516–547.

(6) Dijkmans, J.; Gabriëls, D.; Dusselier, M.; de Clippel, F.; Vanelderen, P.; Houthoofd, K.; Malfliet, A.; Pontikes, Y.; Sels, B. F. Productive Sugar Isomerization with Highly Active Sn in Dealuminated β Zeolites. *Green Chem.* **2013**, 2777–2785.

(7) Moliner, M.; Román-Leshkov, Y.; Davis, M. E. Tin-Containing Zeolites Are Highly Active Catalysts for the Isomerization of Glucose in Water. *Proc. Natl. Acad. Sci.* **2010**, 6164–6168.

(8) Román-Leshkov, Y.; Moliner, M.; Labinger, J. A.; Davis, M. E. Mechanism of Glucose Isomerization Using a Solid Lewis Acid Catalyst in Water. *Angew. Chem. Int. Ed.* **2010**, 8954–8957.

(9) Román-Leshkov, Y.; Davis, M. E. Activation of Carbonyl-Containing Molecules with Solid Lewis Acids in Aqueous Media. *ACS Catal.* **2011**, 1566–1580.

(10) Moliner, M. State of the Art of Lewis Acid-Containing Zeolites: Lessons from Fine Chemistry to New Biomass Transformation Processes. *Dalt. Trans.* **2014**, 4197–4208.

(11) Holm S. M.; Saravanamurugan, S.; Taarning E. Conversion of Sugars to Lactic Acid Derivatives Using Heterogeneous Zeotype Catalysts Conversion of Sugars to Lactic Acid Derivatives Using Heterogeneous Zeotype Catalysts *Science* **2010**, 602–605.

(12) Tolborg, S.; Sádaba, I.; Osmundsen, C. M.; Fristrup, P.; Holm, M. S.; Taarning, E. Tin-Containing Silicates : Alkali Salts Improve Methyl Lactate Yield from Sugars. *ChemSusChem* **2015**, 613–617.

(13) Lew, C. M.; Rajabbeigi, N.; Tsapatsis, M. One-Pot Synthesis of 5-(Ethoxymethyl)Furfural from Glucose Using Sn-BEA and Amberlyst Catalysts. *Ind. Eng. Chem. Res.* **2012**, 5364–5366.

(14) Nikolla, E.; Román-Leshkov, Y.; Moliner, M.; Davis, M. E. "One-Pot" Synthesis of 5-(Hydroxymethyl)Furfural from Carbohydrates Using Tin-Beta Zeolite. *ACS Catal.* **2011**, 408–410.

(15) Dewaele, A.; Meerten, L.; Verbelen, L.; Eyley, S.; Thielemans, W.; Van Puyvelde, P.; Dusselier, M.; Sels, B. Synthesis of Novel Renewable Polyesters and Polyamides with Olefin Metathesis. *ACS Sustain. Chem. Eng.* **2016**, 5943–5952.

(16) Sølvhøj, A.; Taarning, E.; Madsen, R. Methyl Vinyl Glycolate as a Diverse Platform Molecule. *Green Chem.* **2016**, 5448–5455.

(17) Gilkey, M. J.; Xu, B. Heterogeneous Catalytic Transfer Hydrogenation as an Effective Pathway in Biomass Upgrading. *ACS Catal.* **2016**, 1420–1436.

(18) Corma, A.; Nemeth, L. T.; Renz, M.; Valencia, S. Sn-Zeolite Beta as a Heterogeneous Chemoselective Catalyst for Baeyer-Villiger Oxidations. *Nature* **2001**, 423–425.

(19) Yakabi, K.; Milne, K.; Buchard, A.; Hammond, C. Selectivity and Lifetime Effects in Zeolite-Catalysed Baeyer–Villiger Oxidation Investigated in Batch and Continuous Flow. *ChemCatChem* **2016**, 3490–3498.

(20) Yakabi, K.; Mathieux, T.; Milne, K.; López-Vidal, E. M.; Buchard, A.; Hammond, C. Continuous Production of Biorenewable, Polymer-Grade Lactone Monomers through Sn-β-Catalyzed Baeyer–Villiger Oxidation with H_2O_2. *ChemSusChem* **2017**, 3652–3659.

(21) Hammond, C. Intensification Studies of Heterogeneous Catalysts: Probing and Overcoming Catalyst Deactivation during Liquid Phase Operation. *Green Chem.* **2017**, 2711–2728.

(22) Lange, J. P. Renewable Feedstocks: The Problem of Catalyst Deactivation and Its Mitigation. *Angew. Chem. Int. Ed.* **2015**, 13187–13197.

(23) Sádaba, I.; López Granados, M.; Riisager, A.; Taarning, E. Deactivation of Solid Catalysts in Liquid Media: The Case of Leaching of Active Sites in Biomass Conversion Reactions. *Green Chem.* **2015**, 4133–4145.
(24) Héroguel, F.; Rozmysłowicz, B.; Luterbacher, J. S. Improving Heterogeneous Catalyst Stability for Liquid-Phase Biomass Conversion and Reforming. *Chimia* **2015**, 582–591.
(25) Padovan, D.; Tolborg, S.; Botti, L.; Taarning, E.; Sádaba, I.; Hammond, C. Overcoming Catalyst Deactivation during the Continuous Conversion of Sugars to Chemicals: Maximising the Performance of Sn-Beta with a Little Drop of Water. *React. Chem. Eng.* **2018**, 155–163.
(26) Padovan, D.; Parsons, C.; Simplicio Grasina, M.; Hammond, C. Intensification and Deactivation of Sn-Beta Investigated in the Continuous Regime. *Green Chem.* **2016**, 5041–5049.
(27) Osmundsen, C. M.; Holm, M. S.; Dahl, S.; Taarning, E. Tin-Containing Silicates: Structure-Activity Relations. *Proc. R. Soc. A Math. Phys. Eng. Sci.* **2012**, 2000–2016.
(28) Levenspiel, O. *Chemical Reaction Engineering*, *John Wiley & Sons, New York, 3rd edn.* **1999**, ch. 21, p. 473.
(29) Al-Nayili, A.; Yakabi, K.; Hammond, C. Hierarchically Porous BEA Stannosilicates as Unique Catalysts for Bulky Ketone Conversion and Continuous Operation. *J. Mater. Chem. A* **2015**, 1373–1382.
(30) Lari, G. M.; Dapsens, P. Y.; Scholz, D.; Mitchell, S.; Mondelli, C.; Pérez-Ramírez, J. Deactivation Mechanisms of Tin-Zeolites in Biomass Conversions. *Green Chem.* **2016**, 1249–1260.
(31) Bañares, M. A. Operando Methodology: Combination of in Situ Spectroscopy and Simultaneous Activity Measurements under Catalytic Reaction Conditions. *Catal. Today* **2005**, 71–77.
(32) Weckhuysen, B. M. Determining the Active Site in a Catalytic Process: Operando Spectroscopy Is More than a Buzzword. *Phys. Chem. Chem. Phys.* **2003**, 4351–4360.
(33) Chakrabarti, A.; Ford, M. E.; Gregory, D.; Hu, R.; Keturakis, C. J.; Lwin, S.; Tang, Y.; Yang, Z.; Zhu, M.; Banares, M. A.; Wachs I. E.; A Decade+ of Operando Spectroscopy Studies. *Catal. Today* **2017**, 27–53.
(34) Beale, A. M.; van der Eerden, A. M. J.; Kervinen, K.; Newton, M. A.; Weckhuysen, B. M. Adding a Third Dimension to Operando Spectroscopy: A Combined UV-Vis, Raman and XAFS Setup to Study Heterogeneous Catalysts under Working Conditions. *Chem. Commun.* **2005**, 3015–3017.
(35) Chowdhury, A. D.; Houben, K.; Whiting, G. T.; Chung, S.-H.; Baldus, M.; Weckhuysen, B. M. Electrophilic Aromatic Substitution over Zeolites Generates Wheland-Type Reaction Intermediates. *Nat. Catal.* **2018**, 23–31.
(36) Ferrini, P.; Dijkmans, J.; De Clercq, R.; Van de Vyver, S.; Dusselier, M.; Jacobs, P. A.; Sels, B. F. Lewis Acid Catalysis on Single Site Sn Centers Incorporated into Silica Hosts. *Coord. Chem. Rev.* **2017**, 220–255.
(37) Gunther, W. R.; Michaelis, V. K.; Caporini, M. A.; Griffin, R. G.; Román-Leshkov, Y. Dynamic Nuclear Polarization NMR Enables the Analysis of Sn-Beta Zeolite Prepared with Natural Abundance ^{119}Sn Precursors. *J. Am. Chem. Soc.* **2014**, 6219–6222.
(38) Hwang, S. J.; Gounder, R.; Bhawe, Y.; Orazov, M.; Bermejo-Deval, R.; Davis, M. E. Solid State NMR Characterization of Sn-Beta Zeolites That Catalyze Glucose Isomerization and Epimerization. *Top. Catal.* **2015**, 435–440.
(39) Kolyagin, Y. G.; Yakimov, A. V.; Tolborg, S.; Vennestrøm, P. N. R.; Ivanova, I. I. Application Of ^{119}Sn CPMG MAS NMR for Fast Characterization of Sn Sites in Zeolites with Natural ^{119}Sn Isotope Abundance. *J. Phys. Chem. Lett.* **2016**, 1249–1253.
(40) Yakimov, A. V.; Kolyagin, Y. G.; Tolborg, S.; Vennestrøm, P. N. R.; Ivanova, I. I. ^{119}Sn MAS NMR Study of the Interaction of Probe Molecules with Sn-BEA: The Origin of Penta- and Hexacoordinated Tin Formation. *J. Phys. Chem. C* **2016**, 28083–28092.
(41) Hammond, C.; Padovan, D.; Al-Nayili, A.; Wells, P. P.; Gibson, E. K.; Dimitratos, N. Identification of Active and Spectator Sn Sites in Sn-β Following Solid-State Stannation, and Consequences for Lewis Acid Catalysis. *ChemCatChem* **2015**, 3322–3331.
(42) Wolf, P.; Valla, M.; Rossini, A. J.; Comas-Vives, A.; Núñez-Zarur, F.; Malaman, B.; Lesage, A.; Emsley, L.; Copéret, C.; Hermans, I. NMR Signatures of the Active Sites in Sn-β Zeolite. *Angew. Chem. Int. Ed.* **2014**, 10179–10183.
(43) Wolf, P.; Liao, W. C.; Ong, T. C.; Valla, M.; Harris, J. W.; Gounder, R.; van der Graaff, W. N. P.; Pidko, E. A.; Hensen, E. J. M.; Ferrini, P.; Dijkmans, J.; Sels, B.; Hermans, I.; Coperet, C. Identifying Sn Site Heterogeneities Prevalent Among Sn-Beta Zeolites. *Helv. Chim. Acta* **2016**, 916–927.
(44) Wolf, P.; Valla, M.; Núñez-Zarur, F.; Comas-Vives, A.; Rossini, A. J.; Firth, C.; Kallas, H.; Lesage, A.; Emsley, L.; Copéret, C.; Hermans, I. Correlating Synthetic Methods, Morphology, Atomic-Level Structure, and Catalytic Activity of Sn-β Catalysts. *ACS Catal.* **2016**, 4047–4063.
(45) Courtney, T. D.; Chang, C. C.; Gorte, R. J.; Lobo, R. F.; Fan, W.; Nikolakis, V. Effect of Water Treatment on Sn-BEA Zeolite: Origin of 960 cm^{-1}FTIR Peak. *Microporous Mesoporous Mater.* **2015**, 69–76.
(46) Dijkmans, J.; Dusselier, M.; Janssens, W.; Trekels, M.; Vantomme, A.; Breynaert, E.; Kirschhock, C.; Sels, B. F. An Inner-/Outer-Sphere Stabilized Sn Active Site in β-Zeolite: Spectroscopic Evidence and Kinetic Consequences. *ACS Catal.* **2016**, 31–46.
(47) Kulkarni, B. S.; Krishnamurty, S.; Pal, S. Probing Lewis Acidity and Reactivity of Sn- and Ti-Beta Zeolite Using Industrially Important Moieties: A Periodic Density Functional Study. *J. Mol. Catal. A Chem.* **2010**, 36–43.
(48) Yang, G.; Pidko, E. A.; Hensen, E. J. M. Structure, Stability, and Lewis Acidity of Mono and Double Ti, Zr, and Sn Framework Substitutions in BEA Zeolites: A Periodic Density Functional Theory Study. *J. Phys. Chem. C* **2013**, 3976–3986.
(49) Van der Graaff, W. N. P.; Tempelman, C. H. L.; Li, G.; Mezari, B.; Kosinov, N.; Pidko, E. A.; Hensen, E. J. M. Competitive Adsorption of Substrate and Solvent in Sn-Beta Zeolite During Sugar Isomerization. *ChemSusChem* **2016**, 3145–3149.
(50) Moliner, M. State of the Art of Lewis Acid-Containing Zeolites: Lessons from Fine Chemistry to New Biomass Transformation Processes. *Dalt. Trans.* **2014**, 4197–4208.
(51) Boronat, M.; Concepción, P.; Corma, A.; Renz, M.; Valencia, S. Determination of the Catalytically Active Oxidation Lewis Acid Sites in Sn-Beta Zeolites, and Their Optimisation by the Combination of Theoretical and Experimental Studies. **2005**, 111–118.
(52) Li, G.; Pidko, E. A.; Hensen, E. J. M. Synergy between Lewis Acid Sites and Hydroxyl Groups for the Isomerization of Glucose to Fructose over Sn-Containing Zeolites: A Theoretical Perspective. *Catal. Sci. Technol.* **2014**, 2241–2250.
(53) Van der Graaff, W. N. P.; Tempelman, C. H. L.; Li, G.; Mezari, B.; Kosinov, N.; Pidko, E. A.; Hensen, E. J. M. Competitive Adsorption of Substrate and Solvent in Sn-Beta Zeolite During Sugar Isomerization. *ChemSusChem* **2016**, 3145–3149.
(54) Bermejo-Deval, R.; Orazov, M.; Gounder, R.; Hwang, S. J.; Davis, M. E. Active Sites in Sn-Beta for Glucose Isomerization to Fructose and Epimerization to Mannose. *ACS Catal.* **2014**, 2288–2297.
(55) Li, S.; Josephson, T.; Vlachos, D. G.; Caratzoulas, S. The Origin of Selectivity in the Conversion of Glucose to Fructose and Mannose in Sn-BEA and Na-Exchanged Sn-BEA Zeolites. *J. Catal.* **2017**, 11–16.

Glucose upgrading in H_2O/MeOH: ACTIVE AND STABLE

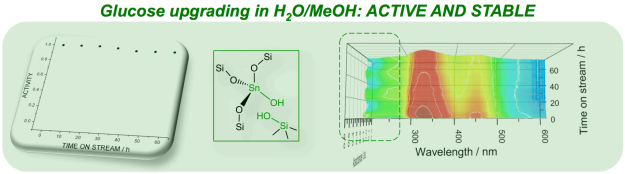

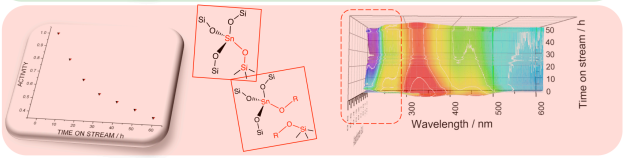

Glucose upgrading in pure MeOH: LOSS OF HYDRATION = DEACTIVATION